JOURNAL OF THERMOPHYSICS AND HEAT TRANSFER
Vol. 9, No. 4, October–December 1995

Constitutive Convolution and Graph Theoretical Representations of Thermodynamic Processes: Thermal Conduction

A. D. Irving*
Rutherford Appleton Laboratory, Oxford, Oxon OX11 0QX, England, United Kingdom
S. J. M. Dudek†
The University of Newcastle, Newcastle Upon Tyne NE1 7RU, England, United Kingdom
T. Dewson‡
University of Bristol, Bristol BS8 1TW, England, United Kingdom
and
G. Warren§
British Gas Plc., Killingworth, Northumberland, England, United Kingdom

It is possible to represent thermodynamic transport processes as either a superposition of constitutive convolution equations in a local region or as a directed graph network between connected regions of the system. Both the local constitutive convolution and directed graph network representations are based on response functions. These response functions for the local constitutive and the Peusner-directed graph network representations can be estimated directly from time series data of the physical observables under general stochastic boundary conditions. The response functions can be used to predict the performance of the materials under a range of external conditions. Both of the representations accurately characterize the future heat flux behavior. However, the main objective of the present work is to determine if the two representations provide physically meaningful and consistent transport coefficient values. The findings of the analyses indicate that only the local constitutive equations yielded the correct values for the physical properties of the materials under test. The nonlinear temporal form of the local constitutive representation is given and then used to estimate the linear and nonlinear thermal conductivity for a range of samples.

Nomenclature

$F_i(t)$ = general thermodynamic force
$H_{J_1J_2}(t)$ = linear impulse response between $J_2(t)$ and $J_1(t)$ in the Peusner-directed graph representation
$H_{J_1\nabla T_2}(t)$ = linear impulse response between $\nabla T_2(t)$ and $J_1(t)$ in the Peusner-directed graph representation
$H_{\nabla T_1 J_2}(t)$ = linear impulse response between $J_2(t)$ and $\nabla T_1(t)$ in the Peusner-directed graph representation
$H_{\nabla T_1 \nabla T_2}(t)$ = linear impulse response between $\nabla T_2(t)$ and $\nabla T_1(t)$ in the Peusner-directed graph representation
$J(t)$ = local heat flux in the constitutive representation
$J_k(t)$ = general thermodynamic flux
$J_1(t)$ = heat flux at surface (1) of a conducting slab of material
$J_2(t)$ = heat flux at surface (2) of a conducting slab of material
$\langle J_2(t - \tau_1)J_1(t)\rangle$ = time-series cross moments between $J_2(t)$ and $J_1(t)$
$\langle J_2(t - \tau_1)J_2(t - \sigma_1)\rangle$ = time-series automoments between $J_2(t)$ and $J_2(t)$
$\langle J_2(t - \tau_1)\nabla T_1(t)\rangle$ = time-series cross moments between $J_2(t)$ and $\nabla T_1(t)$
$\langle J_2(t - \tau_1)\nabla T_2(t - \sigma_1)\rangle$ = time-series automoments between $J_2(t)$ and $\nabla T_2(t)$
L^*_{ijk} = steady-state second-order transport coefficient, $(\partial J_k^2/\partial F_i \partial F_j) = \Sigma^{\mu}_{\sigma_1=0} \Sigma^{\mu}_{\sigma_2=0} L_{J_kF_iF_j}(\sigma_1, \sigma_2)$
L^*_{ik} = steady-state linear transport coefficient, $(\partial J_k/\partial F_i) = \Sigma^{\mu}_{\sigma_1=0} L_{J_kF_i}(\sigma_1)$
$L_{J\nabla T}(t)$ = linear impulse response between $J(t)$ and $\nabla T(t)$ in the local constitutive representation
$L_{J\nabla T\nabla T}(t_1, t_2)$ = second-order impulse response between $J(t)$ and $\nabla T(t)$ in the local constitutive representation
N = order of truncation of the Volterra and Taylor series expansions
θ_1 = first-order steady-state thermal conductivity determined using the local constitutive representation, $\Sigma^{\mu}_{\sigma_1=0} L_{J\nabla T}(\sigma_1)$

Received June 24, 1994; revision received March 27, 1995; accepted for publication April 3, 1995.
*Senior Scientific Officer.
†Senior Lecturer, Department of Building Science.
‡Scientific Officer, Department of Mathematics.
§Statistician.

θ_2 = second-order steady-state thermal conductivity determined using the local constitutive representation $\Sigma_{\sigma_1=0}^{\mu} \Sigma_{\sigma_2=0}^{\mu} L_{J\nabla T \nabla T}(\sigma_1, \sigma_2)$

κ = steady-state thermal conductivity of a solid material

κ_1 = steady-state thermal conductivity determined using the local constitutive representation, $\Sigma_{\sigma_1=0}^{\mu} L_{J\nabla T}(\sigma_1)$

κ_2 = steady-state thermal conductivity determined using the Peusner-directed graph representation, $\Sigma_{\sigma_1=0}^{\mu} H_{J_1 \nabla T_2}(\sigma_1)$

κ_3 = steady-state thermal conductivity determined by the ratio of means method, $|\Sigma_{t=1}^{N} \nabla T(t) / \Sigma_{t=1}^{N} J(t)|$

Λ = number of time-series data points used in the statistical-averaging process

μ = time taken for the system to reach the three half-life decay point after an impulse or step excitation

$\sigma, \sigma_1, \sigma_2, \tau, \tau_1, \tau_2$ = delay with respect to the present time, in units of time

ψ_2 = heat flux gain determined using the Peusner-directed graph representation, $\Sigma_{\sigma_1=0}^{\mu} H_{J_1 J_2}(\sigma_1)$

$\langle * \rangle$ = statistical-averaging operation

$\nabla T(t)$ = local temperature gradient in the constitutive representation

$\nabla T_1(t)$ = temperature gradient at surface (1) of a conducting slab of material

$\nabla T_2(t)$ = temperature gradient at surface (2) of a conducting slab of material

$\langle \nabla T_2(t - \tau_1) J_1(t) \rangle$ = time-series cross moments between $\nabla T_2(t)$ and $J_1(t)$

$\langle \nabla T_2(t - \tau_1) J_2(t - \sigma_1) \rangle$ = time-series automoments between $\nabla T_2(t)$ and $J_2(t)$

$\langle \nabla T_2(t - \tau_1) \nabla T_1(t) \rangle$ = time-series cross moments between $\nabla T_2(t)$ and $\nabla T_1(t)$

$\langle \nabla T_2(t - \tau_1) \nabla T_2 \times (t - \sigma_1) \rangle$ = time-series automoments between $\nabla T_2(t)$ and $\nabla T_2(t)$

$\langle \nabla T_2(t - \tau_1) \nabla T_2(t - \tau_2) \times J_1(t) \rangle$ = time-series third-order cross moments between $\nabla T_2(t)$ and $J_1(t)$

$\langle \nabla T_2(t - \tau_1) \nabla T_2 \times (t - \tau_2) \nabla T_2(t - \sigma_1) \rangle$ = time-series third-order automoments of $\nabla T_2(t)$

$\langle \nabla T_2(t - \tau_1) \nabla T_2 \times (t - \tau_2) \nabla T_2(t - \sigma_1) \nabla T_2(t - \sigma_2) \rangle$ = time-series fourth-order automoments of $\nabla T_2(t)$

$\langle \Pi_{j=1}^{m} F_i(t - \tau_j) \times J_k(t) \rangle$ = general time-series cross moments between $F_i(t)$ and $J_k(t)$

$\langle \Pi_{j=1}^{m} F_r(t - \tau_j) \times \Pi_{i=1}^{n} F_s(t - \sigma_i) \rangle$ = general time-series automoments between $F_r(t)$ and $F_s(t)$

Introduction

REAL thermodynamic systems do not exist in a steady-state world; they respond to the continuously changing environment. To measure the thermal characteristics of real thermodynamic processes the appropriate analysis techniques need to be employed. It is possible to represent thermodynamic problems as either a supposition of local constitutive convolution equations in a local region of the solid or as a directed graph network between connected network regions within the solid. Both the local constitutive convolution and network representations are based on response functions that can, in principle, be used to estimate dynamic transport coefficients of the process. The purpose of this article is to determine if the thermal transport coefficients of the local constitutive and the graph theoretical representations are accurate, consistent, and physically meaningful for a wide range of solid materials.

This work uses novel time-series analysis techniques to determine the thermal characteristics for one-dimensional thermal conduction. An engineering hot box facility with a heat pipe to the external meteorological conditions was used to measure the linear one-dimensional thermal conductivity of a range of homogeneous solid materials. A series of experiments were performed under typical meteorological boundary conditions and the time-series data collected in those experiments was analyzed in the framework of the two representations. The truth model in the present work is the thermal transport coefficients obtained using the ratio of mean's method. Direct comparisons were made with the ratio of mean's thermal conductivity values and the thermal conductivities determined with the two representations. The moment hierarchy method used in the present work to estimate the response function values and the steady-state thermal conductivities is described in detail elsewhere.[1,2] The local constitutive representation is then extended to the mixed linear–nonlinear case. Time-series heat flux and temperature gradient data were analyzed to investigate the degree to which the thermal conduction process may be weakly nonlinear.

Local Constitutive Representation

If it is assumed that the thermodynamic fluxes $[J_k(t)]$ depend on the set of thermodynamic forces $[F_i(t)]$ then each of the thermodynamic fluxes can be written as a multidimensional function of the forces, with

$$J_k(t) = J_k(F_1, \ldots, F_A) \tag{1}$$

This relationship can be defined as an ascending order of a multidimensional Taylor's series expansion[3] with

$$J_k(t) = \sum_i L_{ik}^* F_i(t) + \frac{1}{2!} \sum_i \sum_j L_{ijk}^* F_i(t) F_j(t) + \cdots \tag{2}$$

where the steady-state transport coefficients are given by

$$L_{ik}^* = \left(\frac{\partial J_k}{\partial F_i}\right)_0 \quad \text{and} \quad L_{ijk}^* = \left(\frac{\partial J_k^2}{\partial F_i \partial F_j}\right)_0$$

In both the linear and the nonlinear cases the steady-state transport coefficients are difficult to determine experimentally. The steady-state transport coefficients do not provide any information about the dynamics of the process and their values cannot be derived from purely theoretical grounds. In the linear case, Eq. (2) reduces to the irreversible thermodynamic equations of Onsager.

Equally, the phenomena can be described by an expansion of functionals. If there is a unique solution to the Taylor series expansion then, formally at least, it is the inverse mapping. The emphasis of the inverse problem approach is to identify the form of relationship between the observables, and hence, establish the laws governing the process. For example, $[J_k(t)]$

can be written as a discrete form of the Volterra functional expansion[4] with

$$J_k(t) = \sum_{n=1}^{N} \frac{1}{n!} \sum_{i_1=1}^{I} \cdots \sum_{i_n=i_{n-1}}^{I} \sum_{\sigma_1=0}^{\mu} \cdots \sum_{\sigma_n=0}^{\mu} L_{J_kF_{i_1}\cdots F_{i_n}}(\sigma_1, \ldots, \sigma_n) \prod_{j=1}^{n} F_{i_j}(t-\sigma_j) \quad (3)$$

where N is the order of truncation of the system, where t denotes time, I is the number of forces, and σ_i denotes time delay with respect to t.

The kernel function values $L_{J_kF_{1n}}(\sigma_1, \ldots, \sigma_n)$ characterize the behavior of $[J_k(t)]$ in terms of the forces $[F_1(t)]$. Integrating each kernel function yields the linear and the nonlinear steady-state transport coefficients,[1,2] with

$$L^*_{J_kF_{i_1}\cdots F_{i_n}} = \sum_{\sigma_1=0}^{\mu} \cdots \sum_{\sigma_n=0}^{\mu} L_{J_kF_{i_1}\cdots F_{i_n}}(\sigma_1, \ldots, \sigma_n) \quad (4)$$

For one-dimensional thermal conduction the local heat flux $[J(t)]$ can be expressed as a function of the local temperature gradient $[\nabla T(t) = F_1(t)]$. If the thermal conduction process is assumed to be linear, then the relationship between the heat flux and temperature gradient can be expressed as the convolution[5]

$$J(t) = \sum_{\sigma_1=0}^{\mu} L_{J\nabla T}(\sigma_1)\nabla T(t-\sigma_1) \quad (5)$$

The response function $L_{J\nabla T}(\sigma_1)$ is related to the equilibrium thermal conductivity κ_1 by

$$\kappa_1 = \sum_{\sigma_1=0}^{\mu} L_{J\nabla T}(\sigma_1) \quad (6)$$

As it stands, Eq. (5) is ill-posed, in the sense that there are too many unknown coefficients. This problem can be rectified if a number of independent equations equal to the number of unknown coefficients can be generated. Equation (5) is also usually ill-conditioned, because it has dependent and independent variables that are stochastic functions of time. By operating on Eq. (5) with the averaging operator $\langle \nabla T(t-\tau_1)^* \rangle$ a tractable set of $(\mu + 1)$ equations with well-behaved coefficients is obtained that can be solved for the response function values. In this case the moment hierarchy is given by[1,2]

$$\langle \nabla T(t-\tau_j)J(t)\rangle = \sum_{\sigma_1=0}^{\mu} L_{J\nabla T}(\sigma_1)\langle \nabla T(t-\tau_j)\nabla T(t-\sigma_1)\rangle \quad (7)$$

where this multivariate moment hierarchy is solved by standard matrix methods.

The simultaneous form of the moment equations is more obvious when Eq. (7) is written in matrix form with

$$\begin{vmatrix} \langle \nabla T(t)J(t)\rangle \\ \vdots \\ \langle \nabla T(t-\mu)J(t)\rangle \end{vmatrix} = \begin{vmatrix} \langle \nabla T(t)\nabla T(t)\rangle & \cdots & \langle \nabla T(t)\nabla T(t-\mu)\rangle \\ \vdots & \ddots & \vdots \\ \langle \nabla T(t-\mu)\nabla T(t)\rangle & \cdots & \langle \nabla T(t-\mu)\nabla T(t-\mu)\rangle \end{vmatrix} \times \begin{vmatrix} L_{J\nabla T}(0) \\ \vdots \\ L_{J\nabla T}(\mu) \end{vmatrix} \quad (8)$$

where the cross- and automoments between the observed heat flux $[J(t)]$ and the temperature gradient $[\nabla T(t)]$ are defined as

$$\langle \nabla T(t-\tau_1)J(t)\rangle = \sum_{t=0}^{\Lambda} \nabla T(t-\tau_1)J(t)$$

and

$$\langle \nabla T(t-\tau_1)\nabla T(t-\sigma_1)\rangle = \sum_{t=0}^{\Lambda} \nabla T(t-\tau_1)\nabla T(t-\sigma_1)$$

respectively.

Directed Graph Network Representation

Recently, Peusner[6–9] has developed the thermostatic directed graph network formalism for the multiple thermal subsystem case. In that work the elements of the transfer matrices are assumed to be equal to the partial derivatives of the thermodynamic equations of state when equilibrium conditions prevail, with several thermodynamic variables being assumed to be held at constant values.

Peusner used elements of linear topology and graph theory to develop a directed graph network representation of thermostatic systems. That approach is in direct analogy to the network and graph theoretical methods developed for linear electrical circuits. Kirchhoff's law's are used to obtain a suitable, but not unique,[7] set of equations to describe the thermostatic flows.

Peusner considers a variety of steady-state network forms, in particular, relating the thermodynamic force and flux at each point, with

$$\begin{vmatrix} J_1 \\ F_1 \end{vmatrix} = \begin{vmatrix} H_{J_1J_2} & H_{J_1F_2} \\ H_{F_1J_2} & H_{F_1F_2} \end{vmatrix} \begin{vmatrix} J_2 \\ F_2 \end{vmatrix} \quad (9)$$

In the Peusner thermostatic network representation of a conducting slab of material both surfaces can simultaneously experience unsteady heat flux and temperature gradient conditions. The network equation for the heat flux at one surface $[J_1(t)]$ can be related, by a superposition of convolution equations, to the temperature gradient $[\nabla T_2(t)]$ and the local heat flux $[J_2(t)]$ at the opposite boundary, with

$$\begin{vmatrix} J_1(t) \\ \nabla T_1(t) \end{vmatrix} = \begin{vmatrix} H_{J_1J_2}(\sigma_1) & H_{J_1\nabla T_2}(\sigma_1) \\ H_{\nabla T_1J_2}(\sigma_1) & H_{\nabla T_1\nabla T_2}(\sigma_1) \end{vmatrix} \begin{vmatrix} J_2(t-\sigma_1) \\ \nabla T_2(t-\sigma_1) \end{vmatrix} \quad (10)$$

The equation for the heat flux and temperature gradient are explicitly given by the superposition of two linear convolution terms with

$$J_1(t) = \sum_{\sigma_1=0}^{\mu} H_{J_1J_2}(\sigma_1)J_2(t-\sigma_1) + \sum_{\sigma_1=0}^{\mu} H_{J_1\nabla T_2}(\sigma_1)\nabla T_2(t-\sigma_1) \quad (11)$$

$$\nabla T_1(t) = \sum_{\sigma_1=0}^{\mu} H_{\nabla T_1J_2}(\sigma_1)J_2(t-\sigma_1) + \sum_{\sigma_1=0}^{\mu} H_{\nabla T_1\nabla T_2}(\sigma_1)\nabla T_2(t-\sigma_1) \quad (12)$$

The steady-state thermal conductivity κ_2 and the heat flux gain ψ_2 for the Peusner-directed graph network representation are given by

$$\kappa_2 = \sum_{\sigma_1=0}^{\mu} H_{J_1\nabla T_2}(\sigma_1) \quad \text{and} \quad \psi_2 = \sum_{\sigma_1=0}^{\mu} H_{J_1J_2}(\sigma_1) \tag{13}$$

where, theoretically, $\psi_2 = 1.0$.

The moment equations to be solved for the Peusner response function values are

$$\langle J_2(t-\tau_1)J_1(t)\rangle = \sum_{\sigma_1=0}^{\mu} H_{J_1J_2}(\sigma_1)\langle J_2(t-\tau_1)J_2(t-\sigma_1)\rangle + \sum_{\sigma_1=0}^{\mu} H_{J_1\nabla T_2}(\sigma_1)\langle J_2(t-\tau_1)\nabla T_2(t-\sigma_1)\rangle \tag{14}$$

$$\langle J_2(t-\tau_1)\nabla T_1(t)\rangle = \sum_{\sigma_1=0}^{\mu} H_{\nabla T_1J_2}(\sigma_1)\langle J_2(t-\tau_1)J_2(t-\sigma_1)\rangle + \sum_{\sigma_1=0}^{\mu} H_{\nabla T_1\nabla T_2}(\sigma_1)\langle J_2(t-\tau_1)\nabla T_2(t-\sigma_1)\rangle \tag{15}$$

$$\langle \nabla T_2(t-\tau_1)J_1(t)\rangle = \sum_{\sigma_1=0}^{\mu} H_{J_1J_2}(\sigma_1)\langle \nabla T_2(t-\tau_1)J_2(t-\sigma_1)\rangle + \sum_{\sigma_1=0}^{\mu} H_{J_1\nabla T_2}(\sigma_1)\langle \nabla T_2(t-\tau_1)\nabla T_2(t-\sigma_1)\rangle \tag{16}$$

$$\langle \nabla T_2(t-\tau_1)\nabla T_1(t)\rangle = \sum_{\sigma_1=0}^{\mu} H_{\nabla T_1J_2}(\sigma_1)\langle \nabla T_2(t-\tau_1)J_2(t-\sigma_1)\rangle + \sum_{\sigma_1=0}^{\mu} H_{\nabla T_1\nabla T_2}(\sigma_1)\langle \nabla T_2(t-\tau_1)\nabla T_2(t-\sigma_1)\rangle \tag{17}$$

Ratio of Means Method

In addition to the two time-series representations given earlier, the thermal conductivity of the sample materials is estimated using the ratio of means method. In the ratio of means method steady-state conditions are assumed to prevail and the relationship between the local heat flux and the local temperature gradient will be given by the approximation

$$\sum_{t=1}^{\Lambda} J(t) \approx -\kappa_3 \sum_{t=1}^{\Lambda} \nabla T(t) \tag{18}$$

where Λ is the number of time-series points used to estimate the mean values, and the conductivity from the ratio of means method is κ_3.

Experimental Facility for Low Thermal Conductivity Solid Materials

The heat flux, temperature, and temperature gradients of sample materials were measured in a calibrated hot box arrangement. From these measurements the dynamic and thermal conductivity's response factors are estimated using each of the previous representations for the thermal process. The experimental arrangement shown in Fig. 1 was designed to measure the thermal conductivity of a range of material types.

Essentially, the rig consists of a copper heat pipe to a cold temperature bath that is controlled, and another copper heat pipe to atmospheric conditions that gives a damped stochastic heat flux at the surface of the sample under test. The cold bath is an enclosed copper heat exchanger that has cold water

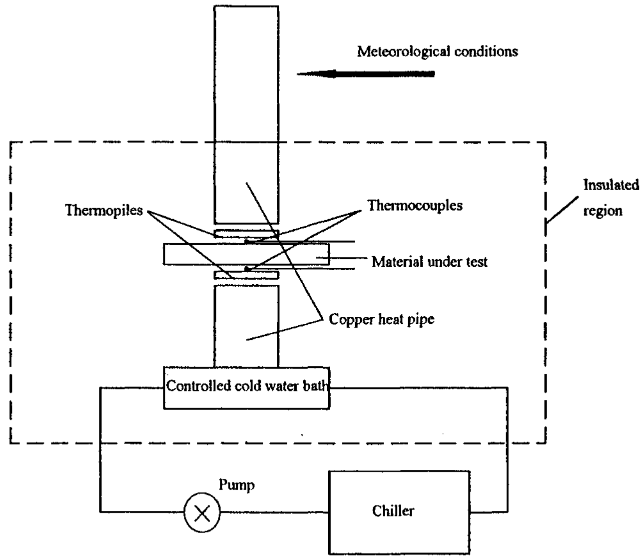

Fig. 1 Schematic diagram of the experimental arrangement.

pumped through it. The absolute temperatures are measured with platinum resistance thermometers and the heat fluxes are measured with thermopiles. The cooling of the water is achieved by using a commercial water chiller. The water is recirculated through the chiller.

The temperature and heat flux are measured at positions above and below the sample as shown in Fig. 1. The test section is surrounded by loose vermiculite insulation. The insulation is contained within a 500-mm^2 enclosure.

The readings were taken every 10 s over an 11-h period, the time interval for data collection was determined by the response time of the sensors used. During the test period 4000 sets of measurements are taken. Of these 4000 points, some 2000 are used to estimate the response function values of the process and the remaining 2000 points are used to compare with the values of the heat flux predicted using the estimated response function values.

Linear Analysis of the Thermal Conductivity Data

These conductivity values, estimated using the local constitutive and the Peusner-directed graph network representations, were compared with the ratio of means values. The estimated response function values obtained using the time-series techniques were then to be used to provide a prediction of $[J_p(t)]$. This prediction was compared with the measured future values of $[J_1(t)]$. This comparison provides a sensitive measure of the quality of the characterization of the thermal transport process. The accuracy of the modeling ability was determined by the students t-test between actual heat flux time-series sequence $[J_1(t)]$ and predicted heat flux time-series sequence $[J_p(t)]$.

In all cases the values of the test statistics for the differences between the measured $[J_k(t)]$ and predicted heat flux $[J_p(t)]$, for both modeled and predicted data, lay well within the acceptance region of the univariate students t-test statistic. Thus, each of the representations accurately quantifies the observed behavior of the heat flux.

The ability to accurately characterize the observed behavior of the process is obviously important. However, the main objective of the present work is to determine if the two representations provide physically meaningful and consistent transport coefficient values. The values of the estimated one-dimensional thermal conductivity from sample material spanning three orders of magnitude are presented in Table 1. Each column contains the values from the analysis of a single sample of time-series data from a single sample of the material. The

Table 1 Estimated thermal conductivities of a range of materials

	Local constitutive	Directed graph network		Ratio of means value
Sample material	κ_1, W/m K	κ_2, W/m K	ψ_2, flux gain	κ_3, W/m K
Stainless steel	12.2 ± 0.36	12.2 ± 0.36	0.0013 ± 0.0004	12.2 ± 0.20
Glass	0.827 ± 0.025	0.078 ± 0.0025	1.007 ± 0.03	0.866 ± 0.040
Glass fiber reinforced polyester	0.191 ± 0.006	0.056 ± 0.0017	0.356 ± 0.011	0.230 ± 0.020
Cork	0.050 ± 0.0015	0.047 ± 0.0015	0.951 ± 0.03	0.049 ± 0.003

Table 2 Estimated thermal conductivity of four different samples of glass

Glass sample	Local constitutive	Directed graph network		Ratio of means value
no.	κ_1, W/m K	κ_2, W/m K	ψ_2, flux gain	κ_3, W/m K
1	0.827 ± 0.025	0.064 ± 0.002	0.949 ± 0.03	0.866 ± 0.040
2	0.611 ± 0.018	0.783 ± 0.022	−0.324 ± 0.011	0.641 ± 0.040
3	0.653 ± 0.019	0.668 ± 0.019	0.002 ± 0.001	0.654 ± 0.040
4	0.720 ± 0.021	0.122 ± 0.004	0.706 ± 0.021	0.740 ± 0.040

Table 3 Estimated thermal conductivity of four different samples of cork

Cork sample	Local constitutive	Directed graph network		Ratio of means value
no.	κ_1, W/m K	κ_2, W/m K	ψ_2, flux gain	κ_3, W/m K
1	0.050 ± 0.0015	0.047 ± 0.0015	0.950 ± 0.100	0.0499 ± 0.0015
2	0.050 ± 0.0015	0.039 ± 0.0012	0.382 ± 0.050	0.0502 ± 0.0015
3	0.050 ± 0.0015	0.044 ± 0.0012	0.135 ± 0.040	0.0504 ± 0.0015
4	0.050 ± 0.0015	0.007 ± 0.0002	1.218 ± 0.040	0.0502 ± 0.0015

fractional uncertainty on the thermal conduction estimated using the ratio of means method is equal

$$\Delta\kappa_3/\kappa_3 \approx \sqrt{(\Delta J_k/J_k)^2 + [\Delta\nabla T(t)/\nabla T(t)]^2} \tag{19}$$

The uncertainties on the thermal conductivity values estimated using the convoltuion equations can be determined by considering the expansion

$$[J_k(t) \pm \Delta J_k(t)] = \sum_{n=1}^{N} \frac{1}{n!} \sum_{i_1=1}^{I} \cdots \sum_{i_n=i_{n-1}}^{I} \sum_{\sigma_1=0}^{\mu} \cdots \sum_{\sigma_n=0}^{\mu} [L_{J_kF_{i_1}\cdots F_{i_n}}(\sigma_1, \ldots, \sigma_n) \pm \Delta L_{J_kF_{i_1}\cdots F_{i_n}}(\sigma_1, \ldots, \sigma_n)] \times \left[\prod_{j=1}^{n} F_{i_j}(t - \sigma_j) \pm \prod_{j=1}^{n} \Delta F_{i_j}(t - \sigma_j)\right] \tag{20}$$

Remembering that $F_{i_j}(t) = \nabla T_{i_j}(t)$ in this case, then for the linear approximation Eq. (20) reduces to

$$[J_k(t) \pm \Delta J_k(t)] = \sum_{i_1=1}^{I} \sum_{\sigma_1=0}^{\mu} [L_{J_kF_{i_1}}(\sigma_1) \pm \Delta L_{J_kF_{i_1}}(\sigma_1)] \times [\nabla T_{i_1}(t - \sigma_1) \pm \Delta\nabla T_{i_1}(t - \sigma_1)] \tag{21}$$

Using the fact that[1]

$$\left(\frac{\partial J_k}{\partial F_i}\right) = \sum_{\sigma_1=0}^{\mu} L_{J_kF_i}(\sigma_1) = \kappa_{ik}$$

and ignoring second-order terms, then the uncertainty $\Delta J_k(t)$ can be written as

$$\Delta J_k(t) = \sum_{i_1=1}^{I} \sum_{\sigma_1=0}^{\mu} [\Delta\nabla T_{i_1}(t - \sigma_1) L_{J_kF_{i_1}}(\sigma_1) + \Delta L_{J_kF_{i_1}}(\sigma_1)\nabla T_{i_1}(t - \sigma_1)] \tag{22}$$

If it is assumed that the uncertainty on each experimentally measured time-series point is a constant equal to the calibration uncertainty, i.e., $\Delta J_k \approx$ const and $\Delta\nabla T_{i_1} \approx$ const; and as the temperature gradient is roughly constant in the present work, i.e., $\nabla T_{i_1}(t) \approx \langle\nabla T_{i_1}(t)\rangle$, then the uncertainty on the integral of the estimated response function values will be approximately equal to

$$\frac{\Delta L^*_{J_kF_{i_1}}}{L^*_{J_kF_{i_1}}} \approx \sqrt{\left(\frac{\Delta J_k}{J_k}\right)^2 + \sum_{i_1=1}^{I}\left(\frac{\Delta\nabla T_{i_1}}{\nabla T_{i_1}}\right)^2} \tag{23}$$

where the square root of the quadrature sum has been used instead of the simple arithmetic sum. However, in the Peusner case, this is a lower bound on the uncertainty because of the conditioning of the matrix. The calibration uncertainties are approximately $(\Delta J_k/J_k) \approx 3\%$ and $(\Delta\nabla T_{i_1}/\nabla T_{i_1}) \approx 1\%$.

The values of the estimated one-dimensional thermal conductivity from four different samples of glass and cork are presented in Tables 2 and 3. Each column contains the values from the analysis of a single sample of 400 points of time-series data from a single sample of the material. The first values in the first row of Tables 2 and 3 are the same as those presented in Table 1.

The values of the estimated one-dimensional thermal conductivity from four different samples of cork are presented in Table 3.

The thermal conductivity values estimated with the local constitutive representation agree with the ratio of means estimates within the experimental uncertainties. The thermal conductivity values estimated with the Peusner representation do not agree with the ratio of means estimates. In addition, the heat flux gain values estimated with the Peusner representation are not consistent and do not correspond to the theoretically expected value of 1.0. This suggests that, for one-dimensional thermal conduction, the Peusner matrix is not well conditioned, perhaps due to a linear dependency between the elements of the matrix.

It is clear that the local constitutive representation gives correct, accurate, and consistent values for the conductivities over the whole range of materials considered. In contrast, although the directed graph network representation does give some correct and accurate conductivities for some materials, it is neither consistent nor accurate for the one-dimensional thermal conductivity problem.

Nonlinear Local Constitutive Relationships

Consider representing a thermodynamic observable, e.g., a flux $[J_k(t)]$ in terms of the local temperature gradient $[F_k(t)]$. $[J_k(t)]$ can be represented as a multidimensional convolution expansion in terms of the thermodynamic force $[F_k(t)]$, which in discrete form is given by

$$J_k(t) = \sum_{n=1}^{N} \frac{1}{n!} \sum_{\sigma_1=0}^{\mu} \cdots \sum_{\sigma_n=0}^{\mu} L_{J_k F^n}(\sigma_1, \ldots, \sigma_n) \prod_{i=1}^{n} F_k(t - \sigma_i) \tag{24}$$

where σ_i denotes time delay with respect to present time t.

In the present work, $[J_k(t)]$ is considered to be a mixed first- and second-order functional of the local $[\nabla T(t)]$, where the convolution relationship is given by

$$J(t) = \sum_{\sigma_1=0}^{\mu} L_{J\nabla T}(\sigma_1)\nabla T(t - \sigma_1) + \sum_{\sigma_1=0}^{\mu} \sum_{\sigma_2=0}^{\mu} L_{J\nabla T\nabla T}(\sigma_1, \sigma_2)\nabla T(t - \sigma_1)\nabla T(t - \sigma_2) \tag{25}$$

The estimated response values $L_{J\nabla T^n}(\sigma_1, \ldots, \sigma_n)$ characterize the heat flux in terms of the thermodynamic force acting. In this case the moment hierarchy is given by[1,2]

$$\left\langle \prod_{j=1}^{m} \nabla T(t - \tau_j) J(t) \right\rangle = \sum_{n=1}^{2} \frac{1}{n!} \sum_{\sigma_1=0}^{\mu} \cdots \sum_{\sigma_n=0}^{\mu} L_{J\nabla T^n}(\sigma_1, \ldots, \sigma_n) \times \left\langle \prod_{j=1}^{m} \nabla T(t - \tau_j) \prod_{i=1}^{n} \nabla T(t - \sigma_i) \right\rangle \tag{26}$$

where this multivariate moment hierarchy is solved by standard matrix methods. The previous formulation is general and can be applied to a wide range of situations. Equation (26) is used later to analyze the thermal conduction process in a solid to indicate if conduction is a linear or a nonlinear process.

The truncated Volterra expansion has been operated on in order to obtain a linear algebraic expression that can be readily solved for the transport coefficients. The moment hierarchy can be written in the obvious form $\boldsymbol{C} = \underline{\underline{M}}\boldsymbol{L}$, where $\underline{\underline{M}}$ is a square matrix whose elements are the automoments of the applied forces, $\boldsymbol{C}$ is a column vector whose elements are the cross moments between the thermodynamic flux and the applied forces, and $\boldsymbol{L}$ is a column vector whose elements are the kernel function values. Given the nature of the time-series data considered and the construction of the moment values used in the moment hierarchy, the rows of $\underline{\underline{M}}$ will be linearly independent of each other and the matrix will usually be nonsingular so that there is a unique solution for $\boldsymbol{L}$.

Nonlinear Analysis of the Thermal Conductivity Data

The thermal conductivity of each sample was determined using linear and mixed linear–nonlinear forms of the local constitutive representation. These estimated values of the response functions are then used to predict the future behavior of the heat flux at the surface of the sample. These predicted heat flux values are then compared with the actual observed values.

The uncertainties on the thermal conductivity values estimated using the convolution equations can be determined using

$$[J_k(t) \pm \Delta J_k(t)] = \sum_{n=1}^{N} \frac{1}{n!} \sum_{\sigma_1=0}^{\mu} \cdots \sum_{\sigma_n=0}^{\mu} [L_{J_k\nabla T\cdots\nabla T}(\sigma_1, \ldots, \sigma_n) \pm \Delta L_{J_k\nabla T\cdots\nabla T}(\sigma_1, \ldots, \sigma_n)] \times \left[\prod_{j=1}^{n} \nabla T(t - \sigma_j) \pm \prod_{j=1}^{n} \Delta\nabla T(t - \sigma_j) \right] \tag{27}$$

Again, it is assumed that $\Delta J_k \approx$ const and $\Delta\nabla T_{i_1} \approx$ const; and as the temperature gradient is approximately a constant in the present work, i.e., $\nabla T_{i_1}(t) \approx \langle \nabla T_{i_1}(t) \rangle$ and as[1]

$$\left(\frac{\partial J}{\partial \nabla T}\right) = \sum_{\sigma_1=0}^{\mu} L_{J\nabla T}(\sigma_1) = \theta_1$$

$$\left(\frac{\partial^2 J}{\partial \nabla T^2}\right) = \sum_{\sigma_1=0}^{\mu} \sum_{\sigma_2=0}^{\mu} L_{J\nabla T\nabla T}(\sigma_1, \sigma_2) = \theta_2$$

Table 4 Linear and nonlinear transport coefficients under equilibrium conditions

Sample material	Linear analysis κ_1, W/m K	Nonlinear analysis linear coefficient θ_1, W/m K	Nonlinear analysis quadratic coefficient θ_2, W/K^2
Stainless steel 1	12.20 ± 0.36	13.05 ± 0.36	−0.0040 ± 0.00014
Stainless steel 2	12.20 ± 0.36	12.17 ± 0.36	−0.031 ± 0.001
Glass 1	0.827 ± 0.025	1.060 ± 0.031	0.030 ± 0.001
Glass 2	0.827 ± 0.025	1.060 ± 0.031	0.030 ± 0.001
Glass fiber reinforced polyester	0.191 ± 0.006	0.0952 ± 0.006	0.00015 ± 0.00005
Glass fiber reinforced polyester	0.190 ± 0.006	0.0954 ± 0.006	0.00014 ± 0.00005
Cork	0.050 ± 0.0015	0.100 ± 0.032	−0.0042 ± 0.0001
Cork	0.050 ± 0.0015	0.101 ± 0.032	−0.0031 ± 0.0001

then the uncertainty on the integral of the estimated response function values will be approximately equal to

$$\Delta\theta_1/\theta_1 \approx \sqrt{(\Delta J_k/J_k)^2 + (\Delta\nabla T/\nabla T)^2} \tag{28}$$

$$\Delta\theta_2/\theta_2 \approx \sqrt{(\Delta J_k/J_k)^2 + (2\Delta\nabla T/\nabla T)^2} \tag{29}$$

The values of the estimated thermal transport coefficients under equilibrium conditions are presented in Table 4.

The local constitutive representation is a polynomial convolution expansion and not a perturbation expansion. The magnitude of the linear and quadratic terms of the mixed linear–quadratic form can be compared by considering the products $\theta_1\langle\nabla T(t)\rangle$ and $\theta_2\langle\nabla T^2(t)\rangle$. Using the transport coefficient values given in Table 4 together with the average temperature gradients it can be shown that the one-dimensional thermal conduction is weakly nonlinear in solid materials over a range of three orders of magnitude of thermal conductivity. The magnitude of the nonlinear component seems to increase as the value of thermal conductivity decreases. However, the edge-loss effects in the experimental design used in the present work become increasingly important as the thermal conductivity decreases. Thus, at present, no clear inferences can be made about this nor to the existence of any nonlinear mathematical relationship.

Conclusions

In this work the thermal transport conductivity for a range of different materials has been determined using the local constitutive and directed graph network representations. Both representations were able to accurately characterize the observed behavior. However, the main objective of the present work is to determine which of the two representations provides physically meaningful and consistent transport coefficient values. The local constitutive representation gave consistent and accurate values for the materials examined. Although the directed graph network and the representation could produce accurate thermal transport coefficient values for some cases, it was shown not to be consistent.

The nature of one-dimensional thermal conduction was then considered. Linear and mixed linear and nonlinear local constitutive representations were used to characterize the conduction process in a range of sample materials. A weak nonlinearity was observed as the thermal conductivity decreased. However, this could be due to edge effects. Thus, at present, no clear inferences can be made about this nor to the existence of any nonlinear mathematical relationship.

Acknowledgments

This work was funded by the U.K. Science and Engineering Research Council.

References

[1]Irving, A. D., "Stochastic Sensitivity Analysis," *Applied Mathematical Modeling*, Vol. 16, Jan. 1992, pp. 3–15.

[2]Irving, A. D., Dewson, T., Hong, G., and Cunliffe, N., "Generalized Response of a Nonlinear System to Stochastic Sequences," *Applied Mathematical Modeling*, Vol. 19, Jan. 1995, pp. 46–55.

[3]Callen, H. B., *Thermodynamics*, Wiley, New York, 1960, pp. 288, 289.

[4]Irving, A. D., Clayton, B. R., and Dewson, T., "Nonlinear Thermoviscoelastic Behaviour," *IUTAM Symposium, Inhomogenity, Anisotropy and Nonlinearity in Solid Mechanics*, edited by D. Parker and A. England, Kluwer, The Netherlands, 1995.

[5]Gurtin, M. E., and Pipkin, A. C., "A General Theory of Heat Conduction with Finite Speed Waves," *Archive for Rational Mechanics and Analysis*, Vol. 31, 1968, p. 113.

[6]Peusner, L., "Network Thermostatics," *Journal of Chemical Physics*, Vol. 83, No. 3, 1985, pp. 1276–1291.

[7]Peusner, L., "A Network Thermostatic Approach to Hill and King-Altman Reaction Diffusion Kinetics," *Journal of Chemical Physics*, Vol. 83, No. 11, 1985, pp. 5559–5566.

[8]Peusner, L., "Global Reaction: Diffusion Coupling and Reprocity in Linear Asymmetric Kinetic Networks," *Journal of Chemical Physics*, Vol. 77, No. 11, 1982, pp. 5500–5507.

[9]Peusner, L., *Studies in Network Thermodynamics*, Elsevier, Amsterdam, 1986.